IEEE Access
Multidisciplinary ⋮ Rapid Review ⋮ Open Access Journal

Received April 22, 2021, accepted April 30, 2021, date of publication May 7, 2021, date of current version May 13, 2021.

Digital Object Identifier 10.1109/ACCESS.2021.3078165

Cross-Layer Design and Performance Analysis for Ultra-Reliable Factory of the Future Based on 5G Mobile Networks

ATHIRAH MOHD RAMLY, (Student Member, IEEE), NOR FADZILAH ABDULLAH, (Member, IEEE), AND ROSDIADEE NORDIN, (Senior Member, IEEE)

Department of Electrical, Electronic, and System Engineering, National University of Malaysia, Bangi 43600, Malaysia

Corresponding author: Nor Fadzilah Abdullah (fadzilah.abdullah@ukm.edu.my)

This work was supported in part by the Center for Research and Instrumentation (CRIM) and the Faculty of Engineering and Built Environment (FKAB), Universiti Kebangsaan Malaysia (UKM), and in part by the Malaysian Ministry of Education and Universiti Kebangsaan Malaysia Research Grant under Grant FRGS/1/2018/ICT03/UKM/02/3.

ABSTRACT To provide a new level of reliability, latency, and support a massive number of users and smart objects, a new 5G multi-services air interface needs to be addressed for the factory of the future (FoF). However, there are limitations in providing connectivity to a dynamic machine in a factory due to several strict industrial automation requirements. In particular, the strict wireless communication latency and reliability requirements are the major challenges to enable the Industry 4.0 vision. In this paper, a PHY-MAC layer cross-layer model that combines a semi-persistent scheduling at the medium access control layer and NOMA at the physical layer has been proposed to address the limitations. The work extensively investigates the performance of the factory of the future with various considerations of 5G spectrums (in this case 3.5 GHz and 28 GHz), speeds and frequency diversity. In addition, the packet error rate (PER), outage probability and throughput in MAC are evaluated in terms of network density deployment (sparse, moderate, dense), different kinds of speed; 0 km/h, 3 km/h, 7 km/h and 10 km/h, under two 5G frequency spectrums. Through extensive simulations, the considered 5G system parameters produced better results in terms of reliability, where the results showed that the frequency diversity outperformed non-diversity by 2 dB. In a sparse network, the PER results showed better results compared to the dense network density by 2 dB (MMSE), 8 dB (LS-Linear) and 2 dB (LS-Spline). Besides that, robotics in sparse network density and stationary exhibited the best PER results, which is as low as 10^{-7}. Moreover, the performance of mid-band frequency outperformed the high-band frequency by 1.8dB (MMSE) in dense condition and 1.5 dB (MMSE) in sparse deployment at PER $= 10^{-6}$. Hence, this study could be a useful insight for the factory of the future services that are utilizing a 5G mid-band spectrum as well as a high-band spectrum.

INDEX TERMS 5G, cross-layer, PHY, MAC, NOMA, semi-persistent, scheduling, smart factory, mmWave.

I. INTRODUCTION

Industrial Revolution 4.0 (IR 4.0) that depends on the massive machine type communication from the 5G triangle is expected to support a massive number of devices with less or no human involvement at all. One of the Fifth Generation (5G) driven use-cases is ultra-reliable and low-latency communication (URLLC), for which the third partnership project (3GPP) and the international mobile telecommunications 2020 and beyond (IMT-2020) set strict latency and reliability standards [1]–[3]. Reliability in communication service is defined as the ability of the communication service to perform as required for a given time interval, under certain conditions. Intelligent Transportation Systems (ITS), smart homes and healthcare surgeries are amongst the prospective applications that can be further explored. 5G will not only enhance the human-centric communication, but also build a new connectivity network for devices, objects, and sensors, such as the Internet of Things (IoT); thanks to these two new communication frameworks,

The associate editor coordinating the review of this manuscript and approving it for publication was Giovanni Pau.

named massive machine-type communication (MTC) and URLLC [4]. In addition, the emergence of the URLLC paradigm is envisaged to enable real-time and dynamic automation control for vertical applications such as utilities, retails etc., as mentioned in [5]. Vertical applications here mean the connection of various processes done by many systems in an indoor factory boundary.

However, there are challenges in the deployment of mMTC and URLLC for wireless factory automation. Factory automation is defined as an automation application in industrial automation branches typically with discrete characteristics of the application to be automated with specific requirements. The said applications require ultra-high reliability and low latency [6]–[8]. For ultra-reliability, the requirement is standardized at 99.99999% or higher, whereas the latency is as low as 1ms [9]. The concept of reliability is that a certain packet from an end device is likely to be transmitted within a predefined delay successfully to another peer device. The most often used performance measurement for reliability is Packet Error Rate (PER) at the MAC layer. The PER requirement in industrial automation can be as low as 10^{-9} [8], [10]–[12] for the case of robotic arms, conveyor systems and driverless autonomous transportation systems. However, the exact requirements on reliability may vary in accordance with the specific scenarios and environments.

Previously, several wireless communication technologies have been introduced and developed for industrial applications. Among the technologies are Industrial WLAN, ZigBee, 6LoWPAN, ultrawideband (UWB), ISA 100.11a, as well as WirelessHART [13]. In an automation system for instance, these communication technologies are used to link sensors, actuators, and controllers. However, these technologies run at an unlicensed spectrum and hence, this causes interference to the shared frequency band. This will then lead to the inability to provide deterministic feedback needed for real-time industrial services. Wireless networking is now mainly used for specialized systems and scenarios, such as in the process industry, or for connecting common IT hardware to a distribution network and other related non-critical applications. On one side, this is because there was no need for wireless communication in the past as manufacturing facilities were relatively stagnant and long-lasting. On the other hand, this is due to the fact that most current wireless technologies fall short of the stringent specifications of industrial applications, especially in terms of end-to-end latency, communication service availability, jitter, and reliability. However, with the arrival of Industry 4.0 and 5G, this will change radically since only wireless networking provides the level of reliability, mobility, usability, and ergonomics needed by the factories of the future. As a result, 5G may have a huge impact on how products are manufactured, delivered, and serviced over their entire lifecycle.

Nonetheless, the cellular technologies introduced by the 3GPP, such as mmWave provides an advantage to the licensed spectrum in industrial wireless communication. However, obstacles faced by the industrial manufacturers such as one worldwide solution has made it difficult to inter-operate between devices of different manufacturers. Intuitively, 3GPP has performed several research studies to fill in the gap needed globally to develop of one standard for industrial wireless communication. Among the studies are latency-critical use-cases, such as real-time VoLTE, TCP based applications, gaming [14]. IMT-2020 has also stated that industrial wireless communication is one of the most crucial use-cases for 5G [15].

Several research studies related to industrial automation with 5G have been validated and published globally. In [16], the authors proposed a comprehensive system level simulation that investigates and compares the performance of LTE and 5G in a factory deployment scenario. On the other hand, authors in [17] presented and investigated the resource allocation mechanisms for reliable communication by using normal cellular as well as device-to-device communication.

Meanwhile, researchers in [18] suggested a pilot-assisted variable rate for the URLLC scheme by evaluating the likelihood of device outage under the proposed scheme, described as the failure of at least one of the receiving nodes, and comparing its output to other benchmark schemes including two-hop/cooperative relay and fixed-rate multi-BS transmission. Over a wide range of payload sizes, the suggested scheme reliably offers ultra-reliable connectivity. On the contrary, authors in [19] have proposed a contention-based transmission scheme with small payload users to achieve targeted reliability and latency performance. Apart from that, the authors in [20] suggested a resource reservation scheme to decrease the random-access delay, which showed that the proposed scheme with separate preamble reservation could achieve the delay requirements of URLLC. However, the paper only focuses on the latency performance and neglects the reliability analysis.

On the other hand, [21] examined the performance of the random-access channel in Narrowband-IoT to support the mMTC. However, the authors did not provide detailed parameters, such as carrier frequency or the payload sizes of the packet. In [22], the authors suggested several reliability enhancement methods by introducing packet redundancy over consecutive subframes and using multiple carriers, which showed a significant 10^{-7} block error rate (BLER) performance. However, the study only considered the LTE Release 14 standard and did not explore the 5G standards. Apart from this, researchers in [23] proposed a control channel design using an appropriate assortment of coding, diversity, modulation, as well as frequency/time resources. Results in [23] showed that QPSK is considered in UL CCH. In addition to that, one resource block bandwidth (RB BW) and 2 OFDM symbols are considered to meet the mMTC requirements. Consequently in [24], the researchers explored techniques to mitigate pilot decontaminate in a 5G system. Meanwhile, the researchers in [25] considered a polar-coded joint-iterative detection and decoding in an SCMA 5G system, where the proposed technique outperformed the conventional separate scheme at the receiver.

The primary motivation for this paper is driven by the emerging 5G technologies as stated in [26], where a multicast control channel along with semi-persistent scheduling that is in line with the conventional cellular systems is considered for wireless factory automation in 5G to enhance the MAC layer performance. One of the critical aspects of mMTC is conveying the scheduling data signals in a strict timely fashion with high reliability. To design the URLLC system, it is essential to explore further and examine the performance of MAC layer transmission of different frequency diversity and channel coding. Subsequently, network deployment design for MAC layer is designed accordingly considering three scenarios: sparse, moderate, and dense number of sensors or robotics in an indoor factory building.

Hence, the main contributions of this paper are as follows:

1. Analysis of data transmission signals in terms of packet error rates (PER), outage probability and throughput at MAC layer based on the inputs from PHY layer of NOMA OFDM-based Polar-Coded Sparse Code Multiple Access (PC-SCMA).
2. Characterization and analysis of a suitable control channel signaling mechanism and the payload demand.
3. A MAC layer system model is designed and developed by introducing an appropriate selection of parameters in terms of channel coding, frequency diversity, and channel estimation techniques.
4. MAC layer performance is based on several network densities deployment (sparse, moderate, and dense), representing the number of sensors/robotics in an indoor industrial wireless communication.
5. Analysis performance comparison in a factory of the future deployment scenario at different 5G spectrums, namely mid-band (3.5 GHz) and high band (28 GHz).
6. The results are also investigated at different speeds to represent various sensors/robotics devices in an indoor factory, from 0 km/h (static), 3 km/h, 7 km/h, and 10 km/h, respectively.

This paper has the following structure. Section I described the research motivation as well as the review of previous related works of the PHY-MAC layer. The basic concept, parameter assumptions as well as the system model are discussed in Section II. The PHY-MAC layer simulation system is analyzed in Section III. Results and discussions are explained in Section IV. Lastly, Section V presented the conclusion of the paper.

II. INDUSTRIAL APPLICATION AND ITS REQUIREMENTS

The main elements of scenarios that necessitate very low latency and high connectivity service availability are explained as follows [27].

1. Factory automation: The communication system in factory automation is subjected to high demands in terms of efficiency and availability. Factory automation systems (discrete) are often installed in geographically restricted locations, with restricted connectivity to authorized users and isolated from other cellular customers' networks or network services.
2. Process automation: The management of processing and handling of substances such as explosives, food, and beverage, is referred to as process automation. System automation increases the efficiency of manufacturing operations, reduces energy consumption, and increases facility safety.
3. HMIs and Production IT: Human-machine interfaces (HMIs) provide a wide range of technologies for interacting with machines and production lines, such as panels connected to machines or production lines, as well as standard IT devices like notebooks, tablets PCs and smartphones.

In this article, communication aspects of a factory automation system are considered. Fig. 1 shows the use-cases analysis of various industrial services with respect to their reliability and latency. Each use-case is categorized into three classes. Class A is stated as less critical services, such as maintenance and diagnostic applications [10]. Meanwhile, Class B is the closed loop application and mission critical industrial application that comes up with a higher demand on latency and reliability, as compared to Class A. Some examples of applications in Class B are production line and machine tools. On the other hand, Class C exhibits similar requirements in terms of reliability with Class B, but it has a much higher demand for latency. Examples of applications in Class C are robots and printing machines. Table 1 below shows the summary of the requirements needed by the industrial automation services.

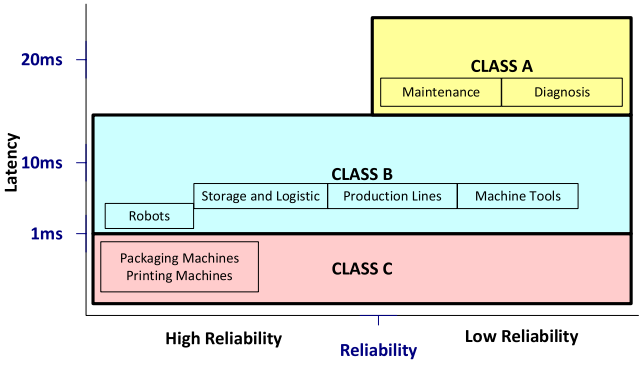

FIGURE 1. Overview and classification of wireless industrial automation services and their requirements.

Based on Table 1, this research paper focuses on class C factory automation, which represents scenarios in real-time, closed loop communication between machines to increase flexibility and efficiency, as mentioned in use-case family 1 in [28]. A highly reliable wireless communication is needed to integrate multiple mobile robots into closed loop communications. Use-case family 1 in [28] envisaged to communicate at low-bitrates but with ultra-high reliability machine-type communication, where convergence and seamless connectivity are required across different radio access technologies.

TABLE 1. Wireless factory automation services requirements [8], [11], [22].

Class	Applications	Latency	PER
A	Diagnostic [7] Maintenance [7]	> 15ms	10^{-4}
B	Machine tools [18][19] Production Lines [7][18][19]	< 15ms	$< 10^{-5}$
C	Robotics [18][19] Printing machines [18][19]	< 7ms	$< 10^{-5}$

There are two common patterns in factory automation. One is open-loop control and the second is closed-loop control. The lack of output control is the most noticeable feature of open-loop control. By delivering desirable output responses to an actuator, it is presumed that the output of the affected phase is predetermined and within an acceptable range [29]. This type of control loop is effective when the effects of the atmosphere on the process and actuator are minimal. This regulation is often used where unwanted output can be accepted.

Closed-loop management applications in industrial factory automation require communications. Motion management of robots, robot arms, packing and printing machines are examples of such applications as shown in Fig 1. A controller interfaces with a significant number of sensors and actuators (up to 100) incorporated in a production unit in motion control applications. Thus, the sensor/actuator density is often very high (up to 1 m^{-3}). Inside a warehouse, these manufacturing units may need to be assisted in close proximity (e.g., up to 100 in automobile assembly line production). In a closed-loop control system, the controller sends periodic commands to a series of sensor/actuator units, which responds within a cycle time. The messages are normally short (56 bytes). The cycle time for message forwarding can be as short as 2 milliseconds, imposing strict end-to-end latency restrictions (1 ms). Additional jitter (1 μs) limitations apply to isochronous message transmission and the communication facility must also be strongly available (99.999999 %) [8]. Multi-robot collaboration is a type of closed-loop control in which a group of robots work together to perform a task, such as symmetrical welding of a car body to reduce deformation. This necessitates all robots operating in perfect agreement. The jitter is one of the command messages of a control case to the community robots for multi-robot cooperation.

The following factors could be necessary to satisfy the rigorous criteria of a closed-loop factory automation:

1. Short-range interactions are limited.
2. For the controller and the actuators, a direct interface link is used.
3. Closed-loop control activities include the use of permitted spectrum. Licensed spectrum can also be used to supplement unlicensed spectrum to improve reliability.
4. Multiple diversity methods in frequency, time, and space can be combined to achieve the high reliability goal under strict end-to-end latency constraints.

The management and regulation of the flow and handling of products and products in industrial production are referred to as logistics and storage. In this regard, intra-logistics is concerned with logistics inside a specific property (e.g., within a factory), such as maintaining the continuous delivery of raw materials on the shop floor level using automated driven vehicles (AGVs), forklifts and etc. This contrasts with logistics between various locations, such as transporting goods from a retailer to a warehouse or from a factory to the end customer. Storage refers to handling of products and goods, which is being more industrialized, for example, with the use of conveyors, cranes, and automated storage and retrieval systems. The localization, recording, and surveillance of assets are critical for all types of logistics applications.

Maintenance and/or diagnosis are the system properties that are monitored without having an immediate effect on the processes themselves. This includes, for example, condition tracking and predictive maintenance based on sensor data, as well as big data analytics for optimizing potential parameter sets of a specific procedure. The data acquisition process is normally not latency-critical for these use-cases, but a large number of sensors will need to be efficiently interconnected, particularly when many of these sensors may be battery-powered.

III. MAC LAYER MODEL

In 5G, the network controls the data signals transmission in uplink and downlink directions. Previously in LTE as stated in [11], the base stations usually monitor the scheduling process. This is due to all the higher layers in the network being removed from the overall network design. There are many benefits of a scheduling-based approach, such as:

1. The network will respond to each user's changing radio situation and maximize the overall throughput.
2. Overload cases can be managed.
3. The network will guarantee each user's QoS.

According to [29], dynamic scheduling is ideal for bandwidth consuming, infrequent and burst signal transmissions. Amongst the applications are e-mails, web-browsing and online streaming. Dynamic scheduling is also not suitable for real-time application voice calls or remote surgeries. To support high capacity and reasonable control signaling, the author in [30] proposed a semi-persistent scheduling which is a combination of dynamic and persistent scheduling [31]. There are two elements in the concept of semi-persistent scheduling: persistent scheduling for initial transmissions and dynamic scheduling for retransmissions. As shown in Fig. 2, UE should send a UL Resource Request (RR) to the next generation nodeB (gNB) at the beginning of each active time. For instance, RR may be submitted on a dedicated RR channel. Upon receipt of the RR, the gNB allocates to the UE a set of transmission time interval

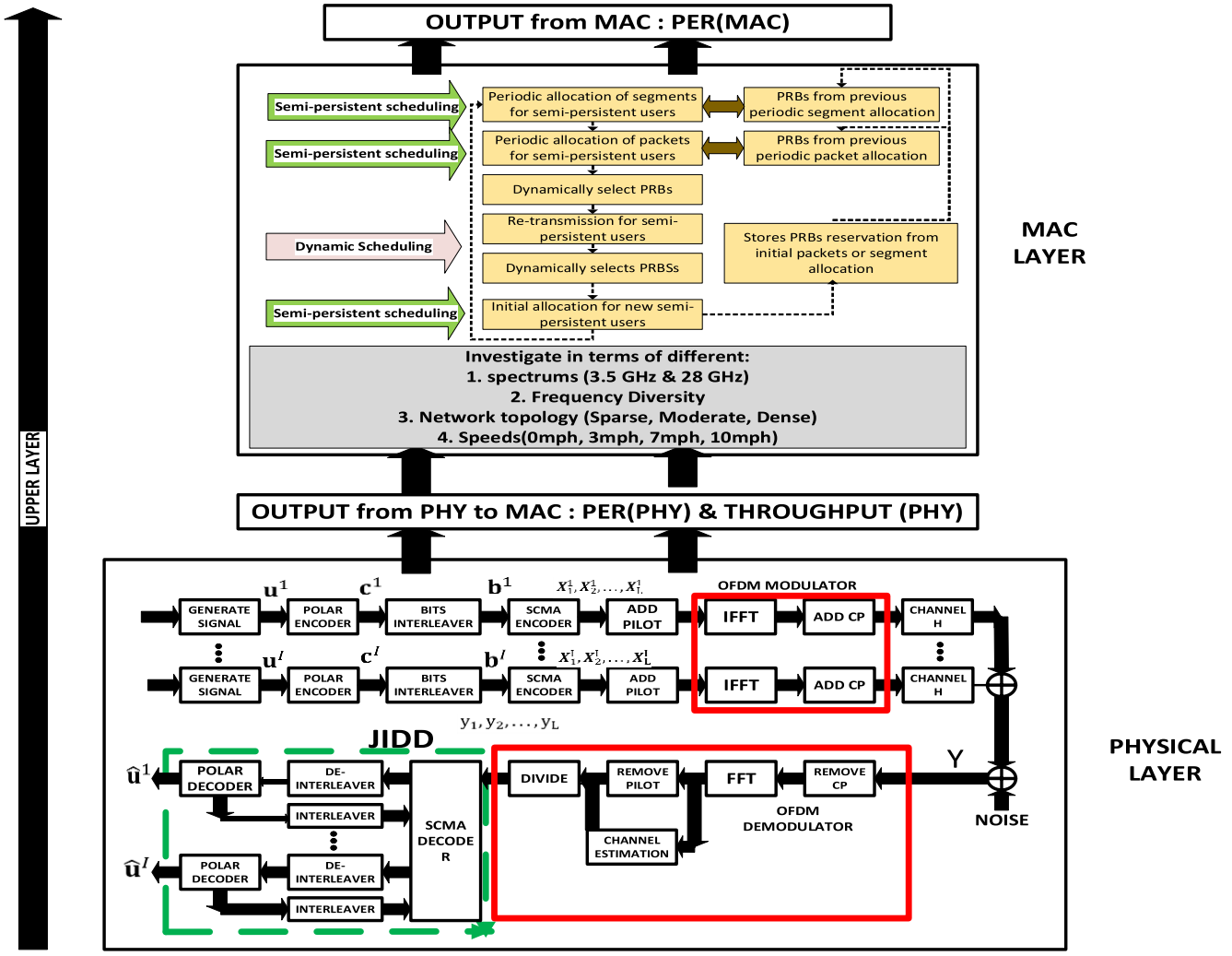

FIGURE 2. PHY-MAC cross layer system model.

resource unit (TTI-RU) chunks placed every 0.1ms, where the UE will transmit all initial transmissions using a pre-assigned transport format. When required, the gNB can reallocate various resources or reassign different transport formats to allow the adaptation of links. The initial transmission allocation is sent to either the control channel PHY (Layer 1) / MAC (Layer 2) or MAC control PDU. The L1 / L2 control channels are used to schedule all the retransmissions dynamically [31].

Due to their infrequent delivery, SID (Silence Insertion Descriptor) packets may be distributed either dynamically or semi-persistently too. The average number of L1 / L2 control channels (N_{CCH}) needed per Transmission Time Interval (TTI) (assuming initial transmissions are planned in a MAC control PDU) if SID packets are dynamically scheduled is [30]:

$$N_{CCH} = \frac{(\lambda - 1)\, nv}{I_1} + \frac{(1 - v)\, n\lambda}{I_2} \tag{1}$$

where n is the number of total users, λ is the average transmission numbers, while I_1 and I_2 denote the inter-arrival time of voice packets and SID packets, respectively.

$$N_{CCH} = \frac{(\lambda - 1)\, nv}{I_1} + \frac{n\,(\lambda - 1)\,(1 - v)}{I_2} \tag{2}$$

To prevent a collision, the transmitting robotic/sensor uses a distributed scheduling mechanism, which involves sensing filled and/or collided resources with other transmitting sensors. Every semi-persistent cycle is sensed by the transmitting sensor, where each transmitting sensor retains its resources for a certain period.

The sensing procedure done by the sensor being transmitted includes [32]:

1. The SCI (control information) transmitted by other vehicles within the sensing range can be decoded by the transmitting sensor and knows which time-frequency resources are assigned to the other sensors.
2. Monitor all available radio services constantly, except for its own. Specifically, the power obtained on each time-frequency resource must be determined to predict

the degree of interference within the resource pool on each time-frequency resource.

Two forms of traffic can occur in a factory automation, which is periodic and sporadic. Semi-Persistent Scheduling (SPS) [30] offers latency advantages for periodic traffic by using previous knowledge of traffic characteristics such as data size and inter-arrival time (or periodicity). As seen in Fig. 3, the scheduling request (SR) and scheduling grant (SG) signaling protocols are conducted once at the initial transmission attempt and the channel resources are then regularly distributed to enable early data transmission. Sporadic traffic, on the other hand, varies greatly from normal traffic because it is of a somewhat irregular sort. Nonetheless, channel capacity can also be pre-allocated to users due to the criticality of those traffic to conduct the necessary data transfer without an additional signaling delay for medium access. Apparently, due to over-provisioning of resources, this occurs at the expense of spectral efficiency.

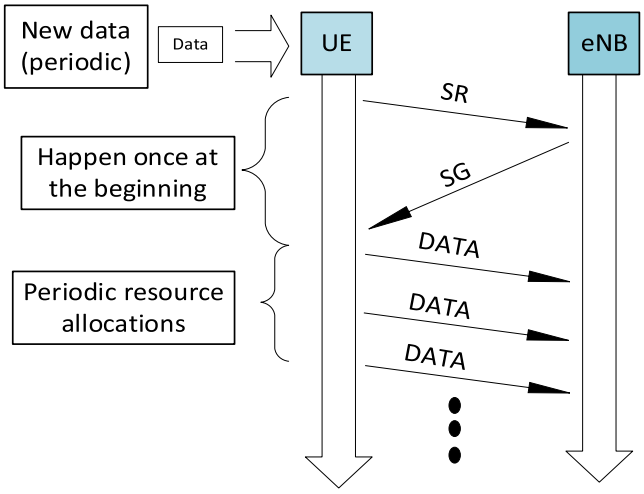

FIGURE 3. Semi-persistent scheduling for indoor wireless automation [11].

A. DIVERSITY

Due to the stringent latency specifications for industrial automation, temporal diversity is insufficient to meet certain factory use-cases, as mentioned in [33]. In this paper, the use-case family 1 [33] is referred to and analyzed for time-critical process optimization for an indoor factory. The use-case in [33] is in line with the objective of the paper, which is to tackle the reliability and increase the efficiency of the production lines. Diversity is one of the most crucial methods to address the ultra-reliability in the wireless industry for FoF. There are several types of diversity, namely spatial, temporal and frequency diversity. In spatial diversity, for example, by installing several antennas on the BS side, we assume that the use of high diversity orders through multiple antennas is practical. Likewise, multiple antennas may be placed on the side of the device, but the number depends heavily on the characteristics of the device. Spatial diversity can be manipulated both at the receiver and/or transmitter side, leading to diversity gains being received and/or transmitted. In addition to gaining diversity gain, transmitting diversity often has an extra receiver processing gain due to the coherent combination of the target signals. In comparison, there would also be an interference rejection gain at the cost of a diversity advantage reduction if spatial degrees of freedom are used to combine interference rejection (IRC). On the other hand, with space-time coding such as Alamouti code, a two-fold diversity order of rate-1 that increases the transmission robustness to multipath fading can be accomplished. FEC coding should be paired with Alamouti code by using more than two transmission antennas to ensure all transmission antennas send the coded bits to influence the decision on a specific information bit [34].

Correspondingly, by assigning the coded bits to several resource blocks (in frequency) with independent channel coefficients, frequency diversity is accomplished. A standard coherence bandwidth of 2-3MHz can be expected in an indoor factory automation environment, as seen in [19]. However, a narrow band of 200 kHz is suggested in this paper, which greatly increases the power usage of user computers, machine capability and spectrum performance to provide both consumer IoT (C-IoT) and mMTC today [9]. Additionally, this paper also focuses on frequency diversity in achieving the reliability of wireless communication in mMTC.

B. RADIO INTERFACE DESIGN AND PARAMETER SIMULATION

We developed an event-based device simulator as in Fig. 4 below to illustrate the ability of the aforementioned radio interface architecture characteristics for ultra-reliable and low-latency communication in a practical factory implementation. The specifics of the factory scenario modelling overview and the simulation assumptions are described below.

1) FACTORY LAYOUT

Simulation experiments were carried out using the deployment of a large factory hall with a height of 12 m, i.e., 1000 m $\times$ 64 m, as seen in Fig. 5. In the center of the factory hall is a 5G base station with a transmitting power of 1 Watt (or 30 dBm). The antenna of the gNB was assumed as an omni-directional antenna and the height of the antenna is placed at 10 m, as considered in [35]. There were six assembly lines (or conveyor belts) within the factory hall. In the plant hall, devices such as sensors and robots were known to be present. The number of devices varies according to certain scenarios.

The three proposed scenarios in the simulation were the users' density in the factory at a time which:

1. *Sparse:* The number of sensors and robotics is set to be 25 per lane per km.
2. *Moderate:* The number of sensors and robotics is set to be 50 per lane per km.
3. *Dense:* The number of sensors and robotics is set to be 100 per lane per km.

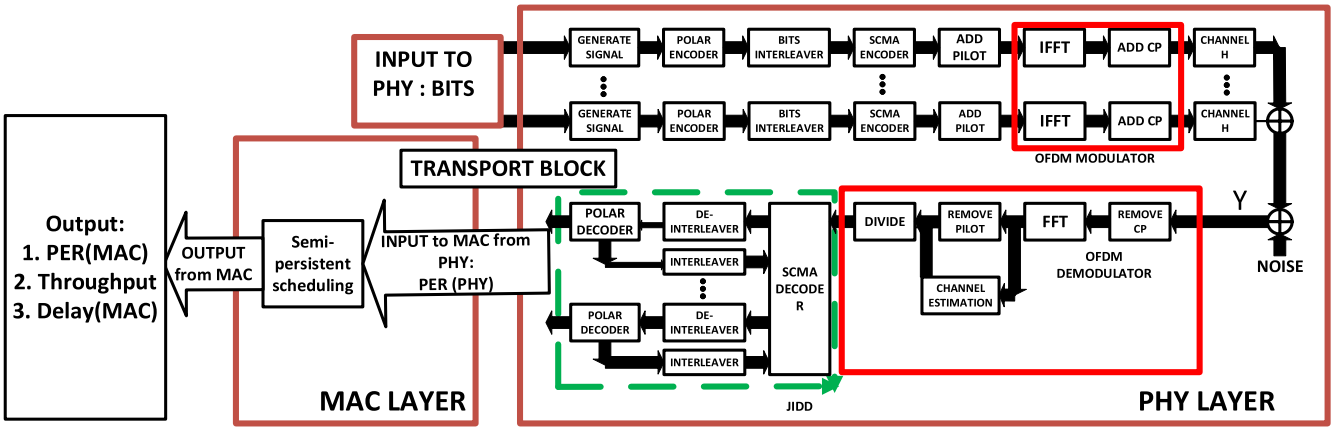

FIGURE 4. Event-based device simulator block diagram scheduling.

2) TRAFFIC MODEL

It is possible to send messages in either a periodic or aperiodic manner. The term ''periodic'' refers to the repetition of a propagation interval. Periodic transmissions may be used to refresh a location regularly or to track a characteristic parameter repeatedly. For example, a temperature transmission every 15 minutes is considered a periodical transmission. However, most periodic intervals in automation communication require very short intervals. Until a stop order is sent, the transmission is initiated once and continues indefinitely.

Meanwhile, an aperiodic transmission is activated instantly by an incident or an event. Events are defined by the control system or by the user. The following are several examples of events:

1. Process events: Process events occur when process limits are crossed or violated, such as temperature, strain, and level, among others.
2. Diagnostic events: Diagnostic events are those that occur when an automated system or module malfunctions, such as a faulty power source, a short circuit, or a temperature that is too extreme.
3. Maintenance events: Maintenance events are triggered by data that shows maintenance work is required to keep an automation system from failing.

In factory communication networks, both periodic and irregular traffic are present. The former is classified as time-triggered traffic with periodically arriving packets. This is due to special occasions such as warnings, hence the latter is activated and occurs sporadically. However, we concentrated mainly on the case of periodic traffic in this article. Since semi-persistent scheduling is introduced in this paper, it is suitable to consider a periodic traffic to exploit the latency advantages by manipulating the previous knowledge about the traffic characteristics. An inter-arrival time of 10ms and a data packet size of 100-bits were considered in this paper. Generally, 100-bits is a typical number of transmission bits in URLLC, as mentioned in [36]. Furthermore, the queue size was assumed to be infinite and hence, the queue can be increased without bound. Besides that, the first-come first-served (FCFS) dispatching discipline was considered in this approach and no items were discarded from the queue. In addition, a M/G/1 queueing model was assumed, in which the arrival rate was Poisson distributed, and the service rate was a general distribution. In the M/G/1 queueing model, the queueing delay, T_w can be expressed as in (3) [37].

$$T_w = \frac{\rho T_s A}{1-\rho} \tag{3}$$

where T_s is the mean service time for each arrival, $\rho = \lambda T_s$ denotes the server load and A represents the scaling factor. Note that the ratio of the standard deviation of service time to the mean ($\sigma Ts/Ts$), known as the variance coefficient, is the main component in the scaling parameter. This provides a normalization calculation of the uncertainty. In our scenario, the value of $\sigma T_s/T_s$ was considered as zero because all the transmitted packets were of the same length.

Additionally, four different mobility speeds traffic were used for evaluation: stationary (0 km/h), 3 km/h, 7 km/h and 10 km/h, respectively. These types of speed ranges were investigated because they were suggested for an indoor environment, as mentioned in [38]–[40]. These speeds are used to analyze the performance behavioral reaction towards different mobility considerations.

3) PROPAGATION MODEL

The frequency of the carrier was proposed to be 3.5 GHz and 28 GHz with a device bandwidth of 200 kHz, which is essential for a reliability analysis [41]. The mid-band range (1-6 GHz) will play a crucial role in the overall deployment of 5G. The 3.5 GHz band for 5G has near-global traction and has already been approved in many countries with another on the way. Technological advances also mean that the 3.5 GHz band will have the same coverage as the existing 2.6 GHz and 1800 MHz satellite bands and use the same cell sites. Meanwhile, the 28 GHz band has been listed as the most likely candidate for 5G ultra-high-speed vision.

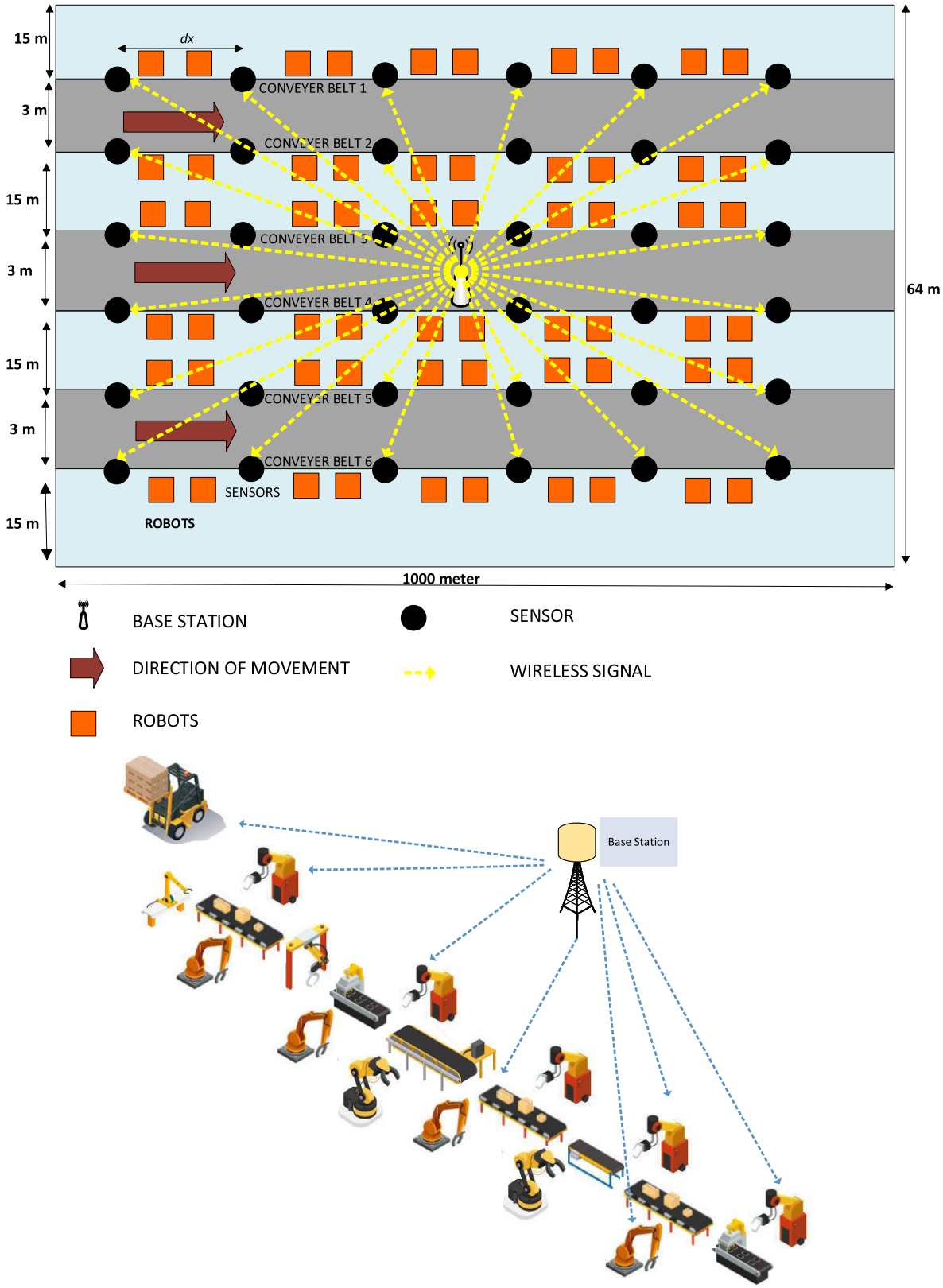

FIGURE 5. Top view design of proposed indoor wireless factory automation (above). Illustration of indoor wireless factory automation (below).

The band of 28 GHz has the advantage of being an adjacent spectrum, enabling economies of scale and promoting the provision of early instruments for all or portions of both bands [9]. Due to the existence of a measurement-based factory propagation model [42], which we regard as the state-of-the-art channel model, an unlicensed frequency range was used. However, since the behavior of the frequency in the adjacent licensed spectrum (e.g., 2 GHz) was not substantially different, the findings presented were still considered true for those frequencies. In general, since the radio channel in the factory setting was dramatically different due to the open floor layout, high ceilings, machinery presence and highly reflective content such as metals, the model also considers fading characteristics of obstructed line-of-sight (OBS). In this case, an OBS loss of 9 dB was proposed.

4) PATH-LOSS MODEL

The sensor/robotics density/m (s_d) and sensor/robotic to sensor/robotic distance (d_{s-s}) were used in the path loss model to calculate the received power $P_R(s,t)$ of each sensor s at a time t according to (4) and (5), where $P_T(s,t)$ is the transmit power, G_T and G_R are transmit and receive antenna gains, L_p is the path loss for indoor industrial[43], whereas X_σ is the shadow fading and n is the pathloss exponent given in Table 2.

$$P_R(s,t) = P_T(s,t) + L_p(s,t) + X_\sigma \tag{4}$$

$$L_p(s,t) = 31.84 + 21.50\log_{10}(d_{s-s}) + 19.00\log_{10}(f_c) \tag{5}$$

The reference sensitivity power level (RX_{sen}) is the minimum mean power applied to the sensor/robotic antenna connector, in which the throughput shall meet or exceed 95% of the maximum throughput of the reference measurement channels [7]. In this work, RX_{sen} given by (7) was used as the minimum received power threshold to sense and predict the interfering sensors/robotics using the same resource. As shown in (6), N_{power} is the noise power calculated from (6) below.

$$N_{Power} = N_{thermal} + 10log(BW) + N_{figure} \tag{6}$$

$$RX_{sen} = N_{Power} + SNR - G_r \tag{7}$$

A list of sensors/robotics *temp* transmits the interfering period messages if their received power $P_R(s,t)$ is greater than (RX_{sen}) as given in (8). Thus, the sum received power of temp sensors ($\sum P_R(temp,t)$ was modelled as an interference in the calculation of $SINR(v,t)$ for each sensor/robotic s at the t in (9), where $ksi\epsilon$ [0,1] is the self-interference cancellation parameter where, $ksi = 0$ corresponds to full cancellation of the self-interference and $ksi = 1$ corresponds to no cancellation.

$$temp = find\,(P_R(s,t) > RX_{sen}) \tag{8}$$

$$SINR(s,t) = P_R(s,t) - [N_{Power} + ksi \times P_T(s,t) + \sum P_R(temp,t)] \tag{9}$$

IV. RESULTS AND DISCUSSIONS

In this section, the results and analysis of the proposed work performance in terms of PER and throughput for various speeds, network density and frequency spectrum were evaluated. The PER output using the OFDM-based PC-SCMA Cross-Layer simulator was stochastically evaluated for at least $N_{iter} = 3000$ for each Signal to Noise Ratio (SNR) value to ensure an acceptable average over the fading phase. All results were obtained using the parameters stated in Table 2 and Algorithm 1 as shown in the previous section.

In Fig. 6(a), (b) and (c), the results shown are the PER results at the PHY layer. The results were analyzed at different frequency diversities and two types of channel estimations were introduced; Minimum Mean Square Error (MMSE) and Least Square (LS) at different interpolation methods; linear and spline. The results showed that PER with frequency diversity had a better performance as compared to the one without diversity. This is due to the spreading of codewords symbols over K resource blocks, which promoted a significant frequency-domain diversity gain.

In addition to that, Fig. 7 showed the performance of PER at the MAC layer of the coded and uncoded OFDM, OFDM-based coded in frequency diversity versus the perfect CSI as a comparison. All the results used MMSE channel estimation as previously, MMSE exhibited better performance than LS in reducing the noise due to the frequency correlation of the LOS Rayleigh fading channel considered. In addition to that, a second-order statistic involved with channel auto-covariance was used in MMSE to reduce the error, as mentioned in [45]. Comparatively, the coded NOMA performance of PER in the MAC layer showed a better per-

Algorithm 1 Semi-Persistent Scheduling in Wireless Factory Automation

1: **for** $i = 1$: (current time/TTI) is integer **do**
2: **for** $i = 1$: (current time/ρ) is integer **do**
3: retrieve cycle and jitter req. of time-triggered
4: M2M devices $d_i, p_i, I\epsilon[1, M]$
5: **if** (obtain minimum Unit Frequency Band (UFB)
6: schedule, $k > k_{max}$) **then**
7: cut the lowest priority device
8: **if** $k < k_{max}$ **then**
9: dynamic scheduling of event triggered M2M
10: devices on bands $[k+1, k_{max}]$
11: **else**
12: semi-persistent scheduling of time triggered
13: M2M device on band $[1, k]$
14: **end if**
15: **end if**
16: retrieve cycle and jitter req. of new
17: time triggered M2M device $d_i, p_i I_\epsilon[1, S]$
18: **break**
19: run call entrance command algorithm
20: **end for**
21: **end for**

TABLE 2. Simulation parameters at PHY-MAC [7], [9], [14], [15], [23], [43], [44].

Parameters	Values
Radio Access Mode (Modulation)	Sparse Code Multiple Access (SCMA)
SCMA codewords	4 OFDMA tones
SCMA codebook size	4
SCMA number of layers	6
Eb/N0	1:20
Channel coding	Polar
Bandwidth (kHz)	200 (NB-IoT)
Scenario	LOS Indoor Factory
Subframe time (ms)	1
Channel Model	Rayleigh fading +AWGN
Receiver Type	MMSE
Carrier frequency (GHz)	3.5/28
Numbers of sensors	48
Numbers of robotics/lane	25/50/100
Traffic Model	Periodic
BS Transmit Power (dBm)	30
Noise Figure (dB)	9
Payload size (bytes)	50/200/300/500
Speeds (for moving robotics) (km/h)	0(static)/3/7/10
Number of Lane	6
Lane width(m)	1
Simulation area size (m)	1000 x 64 x 12
Diversity	Frequency
Subcarrier Spacing (kHz)	60
Symbol duration (μs)	16.67
Cyclic Prefix (μs)	1.17(normal) 17.84(extended)
Subframe (ms)	0.2
Slot (ms)	0.25
Physical channel name	UL
Data rate (kbps)	8.4
Jitter (μs)	100
Delay Spread (DS)	-1.71 ($\mu_{\lg DS}$)
lgDS=$\log_{10}$(DS/1s)	0.18 ($\sigma_{\lg DS}$)
AOD spread (ASD)	1.56 ($\mu_{\lg ASD}$)
lgASD=$\log_{10}$(ASD/1°)	0.25 ($\sigma_{\lg ASD}$)
AOA spread (ASA)	1.66 ($\mu_{\lg ASA}$)
lgASA=$\log_{10}$(ASA/1°)	0.28 ($\sigma_{\lg ASA}$)
Shadow fading (SF) [dB]	4.32
K-factor (K) [dB]	7 (μ_K) 8 (σ_K)
TRANSMITTER	
(1) T_x power (dBm)	23
(2) G_R and G_T (dBi)	8/0
(3) Path Loss Exponent, n	3
RECEIVER	
(2) Thermal noise density (dBm/Hz)	-174
(3) Receiver noise figure (dB)	5
(4) Interference margin (dB)	0
(5) Occupied channel bandwidth (Hz)	200000
(6) Effective noise power = (2) + (3) + (4) + 10 log ((5)) (dBm)	-116
(7) Required SINR (dB)	11
(8) Receiver sensitivity = (6) + (7) (dBm)	-105
(9) Rx processing gain	5
(10) MCL = (1) -(8) + (9) (dB)	133

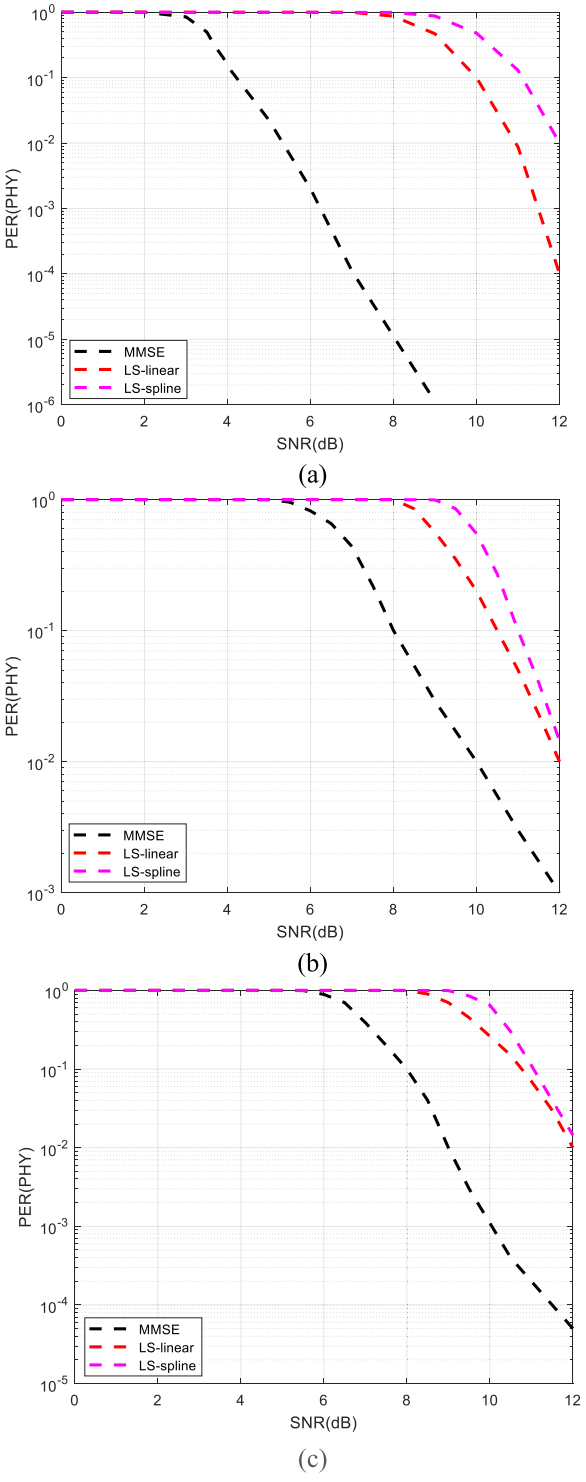

FIGURE 6. PER in PHY layer in rayleigh fading perfect CSI, (b) PER in PHY layer in frequency diversity, (c) PER in PHY layer in rayleigh fading without diversity.

formance than the uncoded ones due to the coded used in the simulator (polar code) helped to mitigate computational complexity at the receiver. Meanwhile, OFDM-based coded NOMA performance of PER in MAC showed the best performance so far. This is due to cyclic prefix at the coding scheme SCMA at PHY layer, which has greatly helped in minimizing the intersymbol interference (ISI). Thus, the combination of

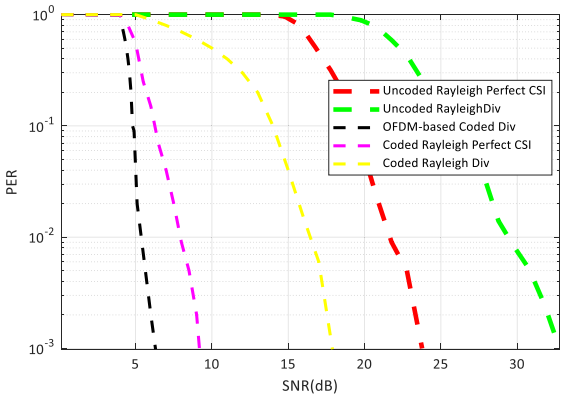

FIGURE 7. Uncoded vs coded vs coded OFDM-based performance comparison in PER.

OFDM-based SCMA with the presence of polar coded has outperformed other results.

On the other hand, Fig. 8 (a), (b) and (c) showed the results of throughput based on results provided from Fig.6 (a), (b) and (c). The throughput was calculated using (9), where R is represented as the error free peak data rate, PER_{phy} is the PER obtained from PHY-layer simulations. It is shown here that MMSE had better performance with perfect CSI and frequency diversity, as compared to non-diversity ones due to the higher root mean square (RMS) delay spread for the channel model in the perfect CSI and frequency diversity.

$$Throughput = R * \left(1 - PER_{phy}\right) \tag{10}$$

In Fig. 9(a), the results were compiled altogether in sparse, moderate, and dense conditions, respectively, by using MMSE and LS estimations (using Spline and Linear interpolation). Fig. 9 (a) and (b) showed the performance results of PER in MAC layer at the frequency spectrum of 3.5 GHz or also known as mid-band 5G in a stationary condition. It showed that PER of MMSE in the perfect channel had the best results compared to the diversity and non-diversity. However, perfect CSI is not realistic since it did not experience any noise in the channel or receiver. Unlike perfect CSI, frequency diversity and non-frequency diversity were simulated in Rayleigh fading with thermal noise. PER with frequency had the PER of 10^{-5}. As shown in Fig. 9 (a), PER was evaluated in 3 conditions: sparse, moderate, and dense network density. It was shown that MMSE with sparse network density in static had the best PER results. The sensor density/meter (v_d) was calculated depending upon the assembly lines configuration values as represented in (11) and (12), where the n is the sensor density/km/lane based on the three seconds rule safe distance between the moving robotic sensors in [38], N_l is the number of lanes shown stated in Table 2.

$$v_d = n * \frac{N_l}{1000} \tag{11}$$

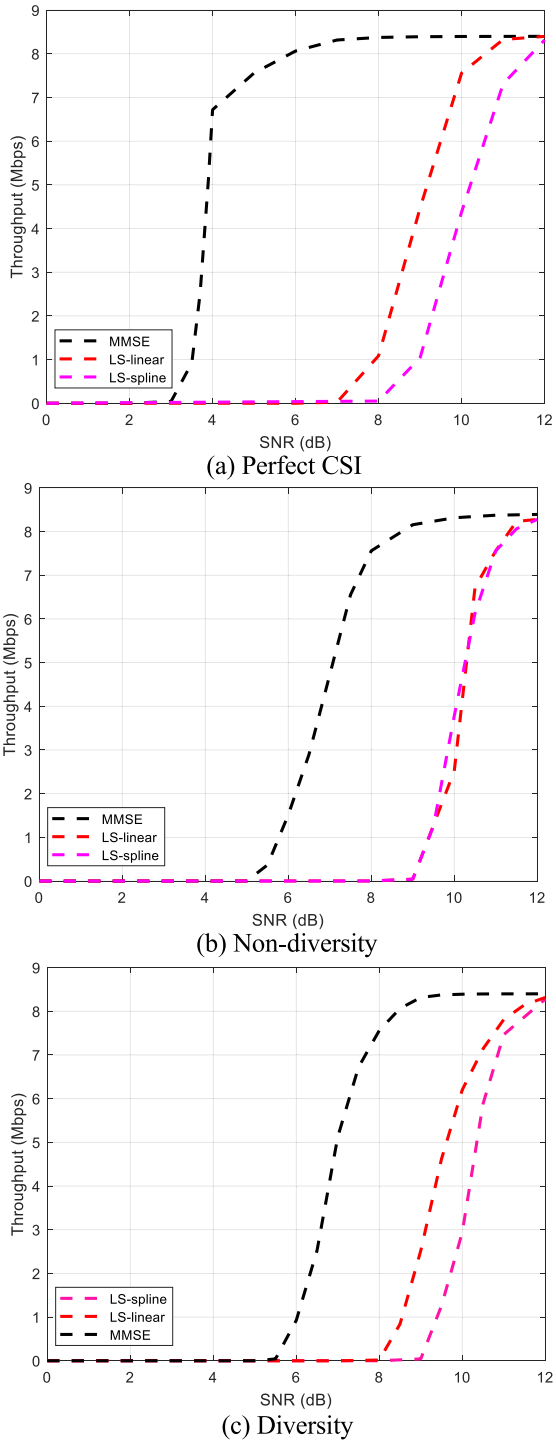

FIGURE 8. Throughput at MAC layer under the moderate density scenario.

$$n = \frac{1000}{6 \times speed} \tag{12}$$

Next, the acceleration of the moving sensors was updated to a new location of the moving robotics and was determined every 0.1 ms using (13), where $[X_t, Y_t]$ were represented the location of the tagged sensors or moving robotics and $[X, Y]$ represented the location of other sensors or robotics.

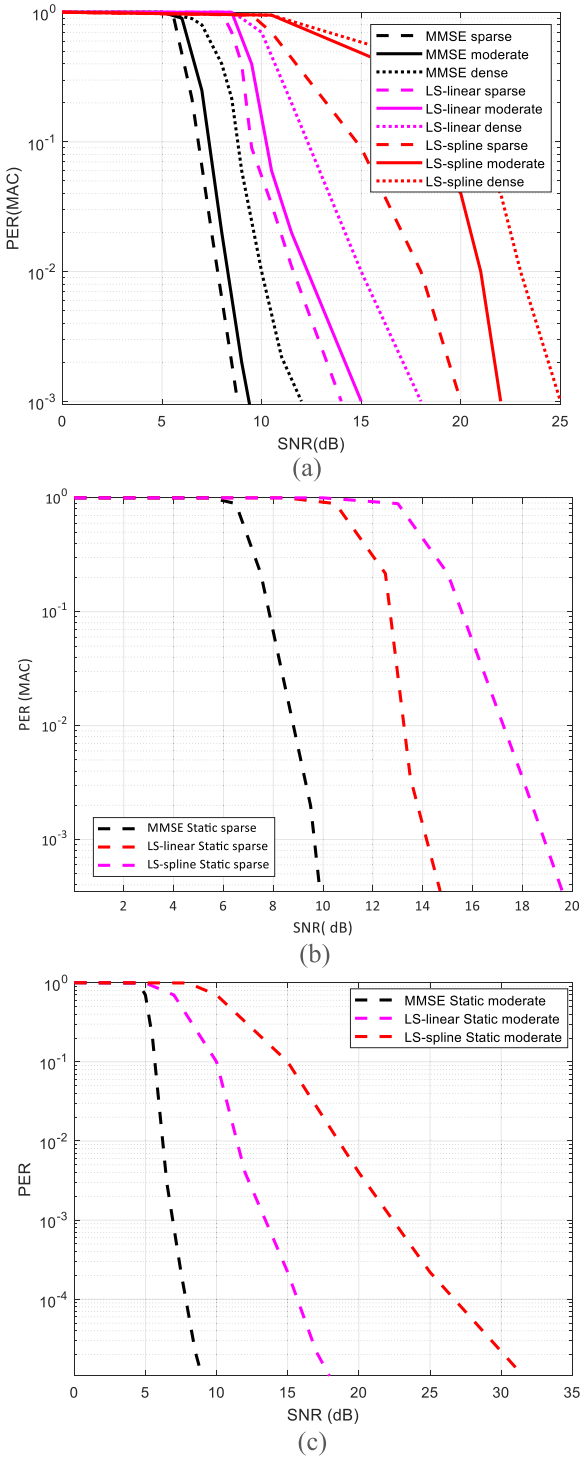

FIGURE 9. PER in MAC layer at the frequency spectrum of 3.5 GHz with (a) frequency diversity and (b) perfect CSI(c) without frequency diversity.

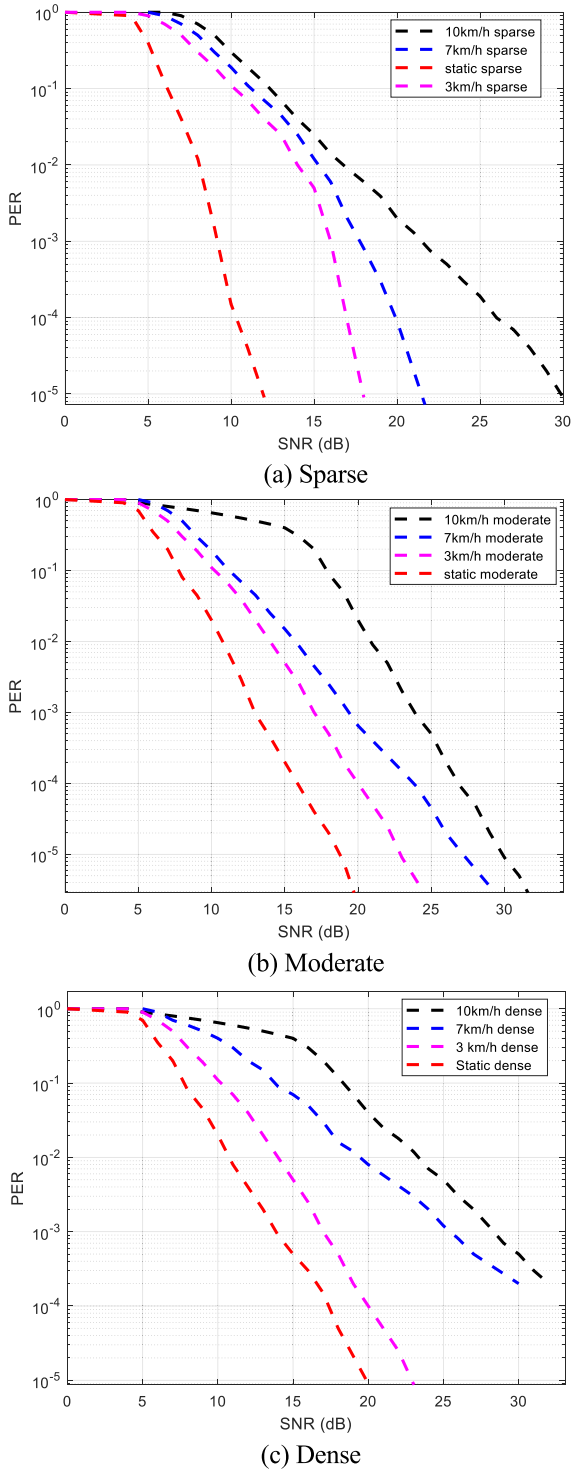

FIGURE 10. PER in MAC layer of different speeds and network densities in frequency diversity.

Then, the received power $P_R(v,t)$ was calculated by using the sensors density and sensor to sensor distance ($d_{(s-s)}$). The $P_R(v,t)$ is the transmit power G_T and G_R are the gain of the transmit and receive antenna and n is the path loss exponent presented in Table 2. Fig. 10(a), (b) and (c) showed that the performance of sparse network density at stationary produced the best overall results compared to the rest with PER lower than 10^{-6}. Meanwhile, a dense network with high mobility displayed the lowest results with high PER.

$$d_{s-s} = \sqrt{(X_t - X)^2 + (Y_t - Y)^2} \tag{13}$$

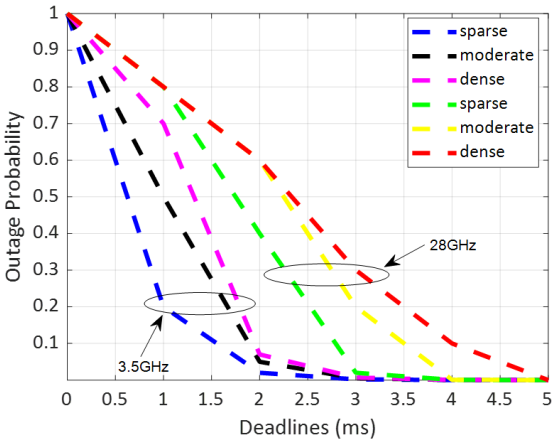

FIGURE 11. Outage probability (in MAC) as a function of time budget in frequency diversity moving at 10km/h.

Fig. 11 illustrated the outage probability versus deadlines. The concept of reliability should relate to the latency specification under the limitations of a URLLC service. When the latency constraint is absent, transmission at a rate lower than the channel capacity ensures perfect reliability. We may characterize the reliability of a communication system with a predefined latency limit as the probability that the latency does not surpass certain deadlines and as the probability of an outage that it does. As mentioned in [28], as a function of the deadlines $R = 1/\tau$ we try to find the maximum coding rate that fits the latency limit $P_r = T_{th}$ in the interest interval of $(0.99 < T_{th} < 0.99999)$. The reliability is $1 - P_{out}$ where P_{out} is the outage probability derived in (14) and (15).

$$\begin{aligned} P_{out}(R) &= P_r\{R > C(h; SNR)\} \\ C(h; SNR) &= log\left(1 + |h|^2 SNR\right) \\ P_{out}(R) &= P_r\left\{R > log(1 + |h|^2 SNR)\right\} \qquad (14) \\ &= P_r\left\{|h|^2 < (2^R - 1)SNR)^{-1}\right\} \\ &= 1 - e^{\frac{-(2^R-1)}{SNR}} \qquad (15) \end{aligned}$$

Since the coding rate equals the opposite of the time threshold as R, the efficiency increased by getting a looser time limit. Thus, the coding rate declined by increasing the deadline and the efficiency is improved since higher coding rates contributed to higher probabilities of an outage and thus lower reliability of communication. This provides the impression that ultra-reliable communication under time diversity is feasible, but it needs a substantial time budget to reach the time limit, which is not a consistent factor with time-critical systems and strict latency specifications.

The results were then further evaluated in different spectrums; 3.5 GHz and 28 GHz, respectively. In Fig. 12 (a), the constant parameters in this graph are the network density and in Rayleigh fading with diversity channel. It was proven that the mid-band 5G outperformed high band 5G in a dense network condition at a speed of 10 km/h in an indoor assembly line. It is stated in [41] that mid-band radios can offer stable

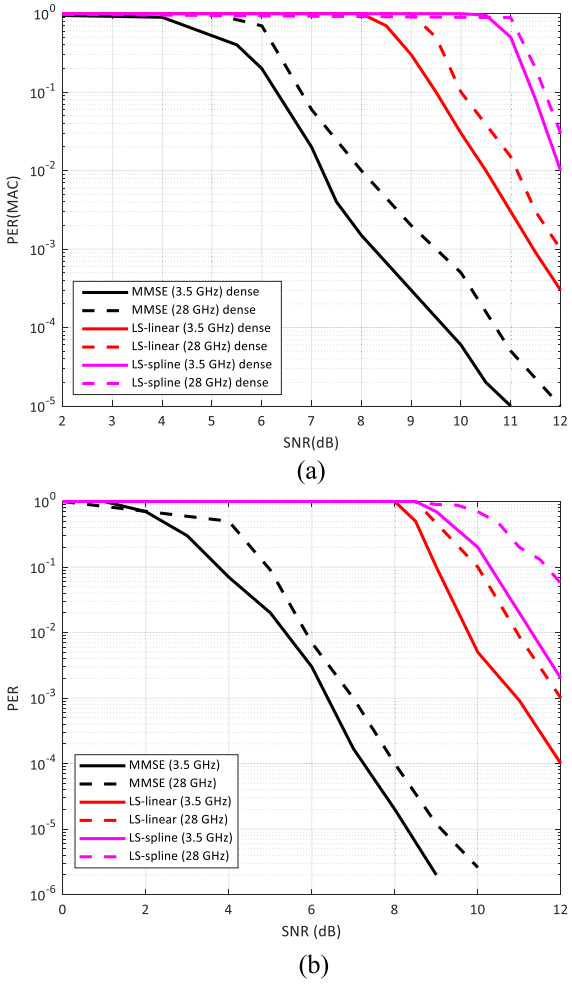

FIGURE 12. PER in MAC Layer of 3.5GHz and 28 GHz in 3 km/h in (a) dense deployment, and (b) sparse network density.

wireless connections within several kilometers radius, further than high-band radios. Unlike mid-band, the high band is able to deliver high speed over short distances and it is highly susceptible to environmental interference from things such as clutter, walls and the number of robotics present in the factory. That is one of the reasons that the mid-band 3.5 GHz spectrum outperformed the high-band results at 28 GHz spectrum, where the mid-band is more robust in a dense network condition, moving in different speed and able to cover a longer radius in a particular environment. The results showed the same impact as mentioned in use-case family 1[1] [46], where it can increase the efficiency of production lines with low bitrates but with ultra-high reliability for real-time closed loop communication such as robot arms and mobile robots [47], [48].

V. CONCLUSION

In this paper, we have designed and developed an indoor factory environment as well as analyzed the overall performance in terms of frequency diversity, network density,

[1]Use-case family 1 refers to time critical process optimization inside factory as mentioned in [46].

device speeds and mid-band and mm-wave band 5G carrier frequency to investigate and address the strict specifications in meeting the 5G requirements for factory automation in a factory environment.

A cross-layer performance in terms of PER and throughput in the MAC layer by using semi-persistent scheduling for indoor Factory of Future (FoF) were evaluated and analyzed. The results showed that the frequency diversity outperformed non-diversity by 2 dB due to the different diversification of the codework spread over the resources. In sparse network density, the PER results showed better results as compared to the dense network density by 2 dB (MMSE), 8 dB (LS-Linear) and 2 dB (LS-Spline) due to the extra overheads incurred in the dense network. The Least Square channel estimate was added and evaluated with the results as a medium of performance comparison.

Subsequently, the performance was further analyzed in terms of speeds. As the speed increased, the PER results heightened due to the Doppler shift and increase in total overheads to the system that occurred during the movement of the sensors/robotics. Robotics in sparse network density and in stationary produced the best results of PER; as low as 10^{-6}. In addition to that, the performance of mid-band frequency outperformed the high-band frequency by 1.8 dB (MMSE) in dense conditions and 1.5 dB (MMSE) in sparse deployment at PER $= 10^{-5}$. This is because the mid-band spectrum offers a stable connectivity in a larger area as compared to the high-band spectrum. Thus, this overall performance analysis stated above might be a useful insight to contribute significant benefits in terms of increased efficiency, and flexibility in services that require high reliability, essentially for the massive machine type communication and mission critical applications.

REFERENCES

[1] S.-Y. Lien, K.-C. Chen, and Y. Lin, "Toward ubiquitous massive accesses in 3GPP machine-to-machine communications," *IEEE Commun. Mag.*, vol. 49, no. 4, pp. 66–74, Apr. 2011, doi: 10.1109/MCOM.2011.5741148.

[2] G. Wu, S. Talwar, K. Johnsson, N. Himayat, and K. D. Johnson, "M2M: From mobile to embedded Internet," *IEEE Commun. Mag.*, vol. 49, no. 4, pp. 36–43, Apr. 2011, doi: 10.1109/MCOM.2011.5741144.

[3] S. R. Pokhrel, J. Ding, J. Park, O.-S. Park, and J. Choi, "Towards enabling critical mMTC: A review of URLLC within mMTC," *IEEE Access*, vol. 8, pp. 131796–131813, 2020, doi: 10.1109/ACCESS.2020.3010271.

[4] D. Feng, C. She, K. Ying, L. Lai, Z. Hou, T. Q. S. Quek, Y. Li, and B. Vucetic, "Toward ultrareliable low-latency communications: Typical scenarios, possible solutions, and open issues," *IEEE Veh. Technol. Mag.*, vol. 14, no. 2, pp. 94–102, Jun. 2019, doi: 10.1109/MVT.2019.2903657.

[5] 5G Americas. (2020). *Mobile Communications Beyond 2020, The Evolution of 5G Towards the Next 5G*. Accessed: Dec. 3, 2020. [Online] Available: https://www.5gamericas.org/wp-content/uploads/2020/12/Future-Networks-2020-InDesign-PDF.pdf

[6] B. Singh, Z. Li, O. Tirkkonen, M. A. Uusitalo, and P. Mogensen, "Ultra-reliable communication in a factory environment for 5G wireless networks: Link level and deployment study," in *Proc. IEEE 27th Annu. Int. Symp. Pers., Indoor, Mobile Radio Commun. (PIMRC)*, Sep. 2016, pp. 1–5, doi: 10.1109/pimrc.2016.7794586.

[7] *Study on Scenarios and Requirements for Next Generation Access Technologies*, document 3GPP TR 38.913 V14.2.0, Mar. 2017.

[8] *Study on Physical Layer Enhancements for NR Ultra-Reliable and Low Latency Case (URLLC)*, document TR 38.824 V2.0.1, 3GPP, Release 16, 2019.

[9] *The National 5G Task Force Report*. Accessed: Dec. 1, 2020. [Online]. Available:https://www.mcmc.gov.my/skmmgovmy/media/General/pdf/The-National-5G-Task-Force-Report.pdf

[10] *Electromagnetic Compatibility and Radio Spectrum Matters (ERM); System Reference Document; Short Range Devices (SRD); Part 2: Technical Characteristics for SRD Equipment for Wireless Industrial Applications Using Technologies Different From Ultra-Wide Band (UWB)*, Standard ETSI TR 102 889-2 V1.1.1, 2011.

[11] 5G Americas. (2020). *New Services and Applications With 5G Ultra-Reliable Low-Latency Communication*. Accessed: Dec. 1, 2020. [Online]. Available: https://www.5gamericas.org/new-services-applications-with-5g-ultra-reliable-lowlatency-communications/

[12] Y. Li, X. Cheng, Y. Cao, D. Wang, and L. Yang, "Smart choice for the smart grid: Narrowband Internet of Things (NB-IoT)," *IEEE Internet Things J.*, vol. 5, no. 3, pp. 1505–1515, Jun. 2018, doi: 10.1109/JIOT.2017.2781251.

[13] D. Christin, P. S. Mogre, and M. Hollick, "Survey on wireless sensor network technologies for industrial automation: The security and quality of service perspectives," *Future Internet*, vol. 2, no. 2, pp. 96–125, Apr. 2010, doi: 10.3390/fi2020096.

[14] *Evolved Universal Terrestrial Radio Access (E-UTRA); Study on Latency Reduction Techniques for LTE (Release 14)*, document 3GPP TR 36.881 (v0.5.0), Jun. 2016.

[15] *ITU Network Standardization Requirements for 5G*. Accessed: Dec. 3, 2020. [Online]. Available: https://www.itu.int/net/pressoffice/press_releases/2015/11.aspx

[16] S. A. Ashraf, I. Aktas, E. Eriksson, K. W. Helmersson, and J. Ansari, "Ultra-reliable and low-latency communication for wireless factory automation: From LTE to 5G," in *Proc. IEEE 21st Int. Conf. Emerg. Technol. Factory Autom. (ETFA)*, Berlin, Germany, Sep. 2016, pp. 1–8, doi: 10.1109/ETFA.2016.7733543.

[17] B. Singh, Z. Li, and M. A. Uusitalo, "Flexible resource allocation for device-to-device communication in fdd system for ultra-reliable and low latency communications," in *Proc. Adv. Wireless Opt. Commun. (RTUWO)*, Riga, Latvia, Nov. 2017, pp. 186–191, doi: 10.1109/RTUWO.2017.8228531.

[18] R. Jurdi, S. R. Khosravirad, and H. Viswanathan, "Variable-rate ultra-reliable and low-latency communication for industrial automation," in *Proc. 52nd Annu. Conf. Inf. Sci. Syst. (CISS)*, Mar. 2018, pp. 1–6, doi: 10.1109/ciss.2018.8362268.

[19] B. Singh, O. Tirkkonen, Z. Li, and M. A. Uusitalo, "Contention-based access for ultra-reliable low latency uplink transmissions," *IEEE Wireless Commun. Lett.*, vol. 7, no. 2, pp. 182–185, Apr. 2018, doi: 10.1109/LWC.2017.2763594.

[20] Y.-J. Chen, L.-Y. Cheng, and L.-C. Wang, "Prioritized resource reservation for reducing random access delay in 5G URLLC," in *Proc. IEEE 28th Annu. Int. Symp. Pers., Indoor, Mobile Radio Commun. (PIMRC)*, Montreal, QC, Canada, Oct. 2017, pp. 1–5, doi: 10.1109/PIMRC.2017.8292695.

[21] R. Harwahyu, R.-G. Cheng, and C.-H. Wei, "Investigating the performance of the random access channel in NB-IoT," in *Proc. IEEE 86th Veh. Technol. Conf. (VTC-Fall)*, Toronto, ON, Canada, Sep. 2017, pp. 1–5, doi: 10.1109/VTCFall.2017.8288195.

[22] I. Aktas, M. H. Jafari, J. Ansari, T. Dudda, S. A. Ashraf, and J. C. S. Arenas, "LTE evolution—Latency reduction and reliability enhancements for wireless industrial automation," in *Proc. IEEE 28th Annu. Int. Symp. Pers., Indoor, Mobile Radio Commun. (PIMRC)*, Montreal, QC, Canada, Oct. 2017, pp. 1–7, doi: 10.1109/PIMRC.2017.8292603.

[23] S. A. Ashraf, F. Lindqvist, R. Baldemair, and B. Lindoff, "Control channel design trade-offs for ultra-reliable and low-latency communication system," in *Proc. IEEE Globecom Workshops (GC Wkshps)*, San Diego, CA, USA, Dec. 2015, pp. 1–6, doi: 10.1109/GLOCOMW.2015.7414072.

[24] M. H. Mazlan, E. Ali, A. M. Ramly, R. Nordin, M. Ismail, and A. Sali, "Pilot decontamination using coordinated Wiener predictor in massive-MIMO system," *IEEE Access*, vol. 6, pp. 73180–73190, 2018, doi: 10.1109/ACCESS.2018.2881743.

[25] Z. Pan, E. Li, L. Zhang, J. Lei, and C. Tang, "Design and optimization of joint iterative detection and decoding receiver for uplink polar coded SCMA system," *IEEE Access*, vol. 6, pp. 52014–52026, 2018, doi: 10.1109/ACCESS.2018.2869906.

[26] M. H. Alsharif, R. Nordin, M. M. Shakir, and A. Mohd Ramly, "Small cells integration with the macro-cell under LTE cellular networks and potential extension for 5G," *J. Electr. Eng. Technol.*, vol. 14, no. 6, pp. 2455–2465, Nov. 2019, doi: 10.1007/s42835-019-00173-2.
[27] *3rd Generation Partnership Project Technical Specification Group Services and System Aspects Study on Communication for Automation in Vertical Domains (Release 16)*, document 3GPP TR 22.804 V16.3.0, Jul. 2020.
[28] P. Nouri, H. Alves, M. A. Uusitalo, O. A. López, and M. Latva-Aho, "Machine-type wireless communications enablers for beyond 5G: Enabling URLLC via diversity under hard deadlines," *Comput. Netw.*, vol. 174, Jun. 2020, Art. no. 107227, doi: 10.1016/j.comnet.2020.107227.
[29] R. C. Dorf and R. H. Bishop, *Modern Control Systems*, 13th ed. Harlow, U.K.: Pearson, 2017.
[30] *Number of Control Symbols*, document 3GPP TSG-RAN WG2 Meeting #57bis, R2-071227 St. Julian's, Malta, Mar. 2007
[31] D. Jiang, H. Wang, E. Malkamaki, and E. Tuomaala, "Principle and performance of semi-persistent scheduling for VoIP in LTE system," in *Proc. Int. Conf. Wireless Commun., Netw. Mobile Comput.*, Shanghai, China, Sep. 2007, pp. 2861–2864, doi: 10.1109/WICOM.2007.710.
[32] *Persistent Scheduling in E-UTRA*, document 3GPP TSG RAN WG1 Meeting #47bis, R1-070098, Sorrento, Italy, Jan. 2007.
[33] 5G Americas. *5G—The Future of IOT*. Accessed: Dec. 1, 2020. [Online]. Available: https://www.5gamericas.org/wp-content/uploads/2019/07/5G_Americas_White_Paper_on_5G_IOT_FINAL_7.16.pdf
[34] 5GPPP. *5G and the Factories of the Future*. Accessed: Dec. 2, 2020. [Online]. Available: https://5g-ppp.eu/wp-content/uploads/2014/02/5G-PPP-White-Paper-on-Factories-of-the-Future-Vertical-Sector.pdf
[35] E. Malkamaki and H. Leib, "Coded diversity on block-fading channels," *IEEE Trans. Inf. Theory*, vol. 45, no. 2, pp. 771–781, Mar. 1999, doi: 10.1109/18.749028.
[36] 5GPPP. *Converged Wireless Access for Reliable 5G MTC for Factories of the Future*. Accessed: Dec. 2, 2020. [Online]. Available: https://5g-ppp.eu/wp-content/uploads/2017/06/Clear5G_Overview_Brussels_5GPPP_Phase2_KickOff.pdf
[37] H. Ren, C. Pan, Y. Deng, M. Elkashlan, and A. Nallanathan, "Joint power and blocklength optimization for URLLC in a factory automation scenario," *IEEE Trans. Wireless Commun.*, vol. 19, no. 3, pp. 1786–1801, Mar. 2020, doi: 10.1109/TWC.2019.2957745.
[38] W. Stallings, *Data and Computer Communications*, 10th ed. London, U.K.: Pearson, 2014.
[39] *Study on Provision of Low-Cost Machine-Type Communications (MTC) User Equipment (UEs) Based on LTE*, document 3GPP TR 36.888 (v0.5.0), Jun. 2013.
[40] *Study on Scenarios and Requirements for Next Generation Access Technologies (Release 14)*, document 3GPP TR 38.913 version 14.2.0, May 2017.
[41] GSMA. *5G Spectrum Positions*. Accessed: Dec. 2, 2020. [Online]. Available: https://www.gsma.com/latinamerica/wp-content/uploads/2019/03/5G-Spectrum-Positions-InfoG.pdf
[42] E. Tanghe, W. Joseph, L. Verloock, L. Martens, H. Capoen, K. Herwegen, and W. Vantomme, "The industrial indoor channel: Large-scale and temporal fading at 900, 2400, and 5200 MHz," *IEEE Trans. Wireless Commun.*, vol. 7, no. 7, pp. 2740–2751, Jul. 2008, doi: 10.1109/TWC.2008.070143.
[43] document 3GPP TSG RAN Meeting #85 RP-191819, Newport Beach, USA, Sep. 2019.
[44] M. Behjati, M. H. Mazlan, A. M. Ramly, R. Nordin, and M. Ismail, "What is the value of limited feedback for next generation of cellular systems?" *Wireless Pers. Commun.*, vol. 110, no. 3, pp. 1127–1142, Feb. 2020, doi: 10.1007/s11277-019-06777-1.
[45] A. Sahu and A. Khare, "A comparative analysis of LS and MMSE channel estimation techniques for MIMO-OFDM system," *Int. J. Eng. Res. Appl.*, vol. 4, no. 6, pp. 162–167, Jun. 2014.
[46] *Cellular System Support for Ultra-Low Complexity and Low Throughput Internet of Things (CIoT) (Release 13)*, document 3GPP TR 45.820 (v13.1.0), Nov. 2015.
[47] A. H. Kelechi, M. H. Alsharif, A. M. Ramly, N. F. Abdullah, and R. Nordin, "The four-C framework for high capacity ultra-low latency in 5G networks: A review," *Energies*, vol. 12, no. 18, p. 3449, Sep. 2019, doi: 10.3390/en12183449.
[48] M. H. Alsharif and R. Nordin, "Evolution towards fifth generation (5G) wireless networks: Current trends and challenges in the deployment of millimetre wave, massive MIMO, and small cells," *Telecommun. Syst.*, vol. 64, no. 4, pp. 617–637, Apr. 2017, doi: 10.1007/s11235-016-0195-x.

ATHIRAH MOHD RAMLY (Student Member, IEEE) received the B.Eng. degree in communication and the M.Sc. degree in communication engineering from International Islamic University Malaysia (IIUM), in 2014 and 2017, respectively. She is currently pursuing the Ph.D. degree with the Department of Electrical, Electronic, and Systems Engineering, Universiti Kebangsaan Malaysia. Her research interest includes wireless communications.

NOR FADZILAH ABDULLAH (Member, IEEE) received the B.Sc. degree in electrical and electronics from Universiti Teknologi Malaysia, in 2001, the M.Sc. degree (Hons.) in communications engineering from The University of Manchester, U.K., in 2003, and the Ph.D. degree in electrical and electronic engineering from the University of Bristol, U.K., in 2012. She is currently an Associate Professor with the Department of Electrical, Electronic, and Systems Engineering, Universiti Kebangsaan Malaysia. Her research interests include 5G, millimeter wave, vehicular networks, MIMO, space time coding, fountain code, and channel propagation modeling and estimation.

ROSDIADEE NORDIN (Senior Member, IEEE) received the B.Eng. degree from Universiti Kebangsaan Malaysia, in 2001, and the Ph.D. degree from the University of Bristol, U.K., in 2011. He is currently an Associate Professor with the Department of Electrical, Electronic, and Systems Engineering, Universiti Kebangsaan Malaysia. His research interest includes the design and analysis of potential physical (PHY) layer transmission technologies for next-generation wireless communication systems.